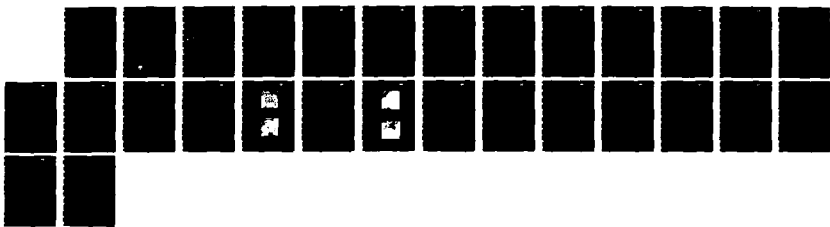
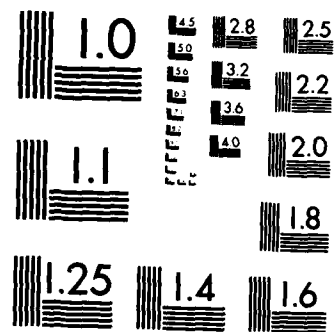


AD-A172 558

LOW DENSITY CERAMICS BASED ON OPEN CELL MACROSTRUCTURES 1/1
FABRICATED FROM R (U) ROCKEELL INTERNATIONAL THOUSAND
OAKS CA SCIENCE CENTER F F LANGE ET AL JUN 86
SC5364 2FR AFOSR-TR-86-0844 F/G 11/2 NL

UNCLASSIFIED





MICROCOPY RESOLUTION TEST CHART
NATIONAL BUREAU OF STANDARDS-1963-A

SC5364.2FR

SC5364.2FR

Copy No. 2

LOW DENSITY CERAMICS BASED ON OPEN CELL MACROSTRUCTURES FABRICATED FROM RETICULATED POLYMER SUBSTRATES

AD-A172 558

FINAL REPORT FOR THE PERIOD
May 1, 1983 through April 30, 1985

CONTRACT NO. F49620-83-C-0078

Approved for public release;
distribution unlimited.

Prepared for

AFOSR
Directorate of Chemical and Atmospheric Sciences
Building 410
Bolling AFB, DC 20332

F.F. Lange
K.T. Miller

JUNE 1986

Approved for public release; distribution unlimited

DTIC FILE COPY



Rockwell International
Science Center

LECT

OCT 1 1986

A

AIR FORCE OFFICE OF SCIENTIFIC RESEARCH (AFSC)
NOTED FOR PUBLIC RELEASE
This technical report has been reviewed and is
approved for public release IAW AFR 190-12.
Distribution is unlimited.
J. K. KETTER
Chief, Technical Information Division

86 10 01 147

UNCLASSIFIED

SECURITY CLASSIFICATION OF THIS PAGE

REPORT DOCUMENTATION PAGE

1a. REPORT SECURITY CLASSIFICATION UNCLASSIFIED		1b. RESTRICTIVE MARKINGS #172558	
2a. SECURITY CLASSIFICATION AUTHORITY		3. DISTRIBUTION/AVAILABILITY OF REPORT Approved for public release; Distribution unlimited	
2b. DECLASSIFICATION/DOWNGRADING SCHEDULE		5. MONITORING ORGANIZATION REPORT NUMBER(S) AFOSR-TR-86-0844	
4. PERFORMING ORGANIZATION REPORT NUMBER(S) SC5364.2FR		7a. NAME OF MONITORING ORGANIZATION AFOSR	
6a. NAME OF PERFORMING ORGANIZATION ROCKWELL INTERNATIONAL SCIENCE CENTER	6b. OFFICE SYMBOL (If applicable) NC	7b. ADDRESS (City, State and ZIP Code) Bldg. 410 Bolling AFB, DC 20332	
8a. NAME OF FUNDING/SPONSORING ORGANIZATION AFOSR	8b. OFFICE SYMBOL (If applicable) NC	9. PROCUREMENT INSTRUMENT IDENTIFICATION NUMBER F49620-83-C-0078	
8c. ADDRESS (City, State and ZIP Code) Bldg. 410 Bolling AFB, DC 20332		10. SOURCE OF FUNDING NOS.	
		PROGRAM ELEMENT NO. 61102F	TASK NO. A3
11. TITLE (Include Security Classification) Microstructural Engineering of Lightweight Ceramic Structures		PROJECT NO. 2303	WORK UNIT NO.
12. PERSONAL AUTHOR(S) Lange / Miller			
13a. TYPE OF REPORT Final	13b. TIME COVERED FROM 01/05/83 TO 04/85	14. DATE OF REPORT (Yr., Mo., Day) June 1986	15. PAGE COUNT 26
16. SUPPLEMENTARY NOTATION			
17. COSATI CODES		18. SUBJECT TERMS (Continue on reverse if necessary and identify by block number)	
FIELD	GROUP	SUB. GR.	
19. ABSTRACT (Continue on reverse if necessary and identify by block number) Processing procedures, and resulting mechanical properties, of open cell low density (relative density less than 0.1) ceramic macrostructures were investigated. These macrostructures were fabricated by slurry coating reticulated polymer substrates. Cracks in the powder coating, which were produced during the pyrolysis of the substrate, remained after powder densification at high temperatures and were the major cause of suboptimum properties. Additionally, lack of slurry drainage during the coating process could fill cells with powder which would differentially shrink during densification, leaving large regions within the macrostructure void of cell struts. This problem became increasingly pronounced with decreasing cell size. Mechanical properties were measured for a commercial transformation toughened Al2O3/ZrO2 based celled material fabricated using reticulated polymer substrates with cell sizes of 30, 65, and 100 pores per inch. Approximately half of the specimens were treated by the manufacturer in an attempt to heal the partially cracked struts. The relative density			
20. DISTRIBUTION/AVAILABILITY OF ABSTRACT UNCLASSIFIED/UNLIMITED <input checked="" type="checkbox"/> SAME AS RPT. <input type="checkbox"/> DTIC USERS <input type="checkbox"/>		21. ABSTRACT SECURITY CLASSIFICATION Unclassified	
22a. NAME OF RESPONSIBLE INDIVIDUAL Dr. Donald Ulrich		22b. TELEPHONE NUMBER (Include Area Code)	22c. OFFICE SYMBOL NC

DD FORM 1473, 83 APR

EDITION OF 1 JAN 73 IS OBSOLETE.

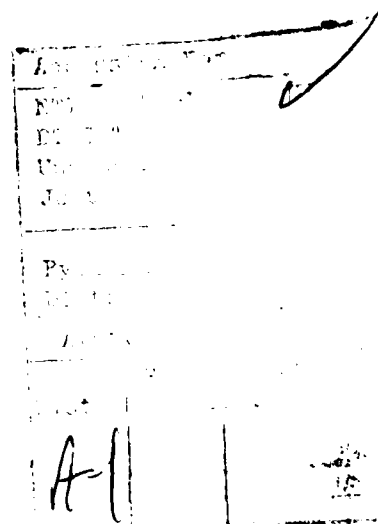
SECURITY CLASSIFICATION OF THIS PAGE

of all commercial materials ranged between 7 and 12% of theoretical. Mechanical properties appeared to be independent of cell size. The elastic modulus, which ranged between 1 and 5 GPa, increased with density and was higher for the "healed" materials. The critical stress intensity factor ranged between 10 and 80 kPam^{1/2}, increasing with elastic modulus. Tensile strength ranged from 0.1 to 0.8 MPa and appeared to be related to processing variations and defects, which included specimen to specimen density variations, cracks within the cell struts and large regions of missing cells in the material with the smallest cell size.



TABLE OF CONTENTS

	Page
1.0 INTRODUCTION.....	1
2.0 EXPERIMENTAL PROCEDURE.....	5
2.1 Fabrication of Reticulated Macrostructures.....	5
2.2 Property Determinations.....	5
3.0 RESULTS.....	8
3.1 Fabrication of Reticulated Macrostructures.....	8
3.1.1 Pyrolysis of Polyurethane Foams.....	8
3.1.2 Slurry Formulation.....	9
3.1.3 Substrate Coating Method.....	9
3.1.4 Densification of Ceramic Macrostructures.....	10
3.2 Properties of the Ceramic Reticulated Macrostructures.....	12
3.2.1 Elastic Modulus.....	12
3.2.2 Fracture Toughness.....	15
3.2.3 Tensile Strength.....	15
4.0 DISCUSSION.....	18
5.0 ACKNOWLEDGEMENTS.....	19
6.0 REFERENCES.....	20





LIST OF FIGURES

<u>Figure</u>		<u>Page</u>
1	Weight loss as a function of temperature (heating rate = 5°C/min) for pyrolysis of polyurethane foam in air.....	8
2	Microstructure of a densified Al ₂ O ₃ /50 vol% ZrO ₂ strut.....	11
3	Macrostructure of a typical open cell reticulated ceramic fabricated using the slurry method.....	11
4	Partial cracks in a reticulated ceramic strut caused by substrate pyrolysis.....	13
5	Macrostructure of a commercially fabricated "healed" reticulated ceramic. Note the second ceramic layer caused by the recoating of the macrostructure.....	13
6	Elastic modulus as a function of relative density for commercial "healed" and "as-received" 65 ppi materials.....	15
7	Fracture toughness as a function of elastic modulus for all commercial specimens.....	16
8	Strength as a function of fracture toughness for all commercial specimens.....	17



LIST OF TABLES

<u>Table</u>		<u>Page</u>
1	Elastic Modulus Values for Each Specimen Set.....	14
2	Relative Density Values for Each Specimen Set.....	14
3	Fracture Toughness Values for Each Specimen Set.....	16
4	Tensile Strength Values for Each Specimen Set.....	17



1.0 INTRODUCTION

Low density ceramics (relative densities < 0.1) are prime candidates for many aerospace applications, ranging from the insulating component of thermal protection systems (e.g., Space Shuttle Tile) to the reinforcement phase in structural composites (e.g., polymer or metal infiltrated systems). Ceramics in the density range of interest may be fabricated into four basic macrostructures: tangled fiber networks, "particulate" networks, closed cell structures, and open cell structures.

Tangled fiber networks are generally fabricated by slurry mixing fibers with a high temperature binding agent (e.g., an alkoxide). The fibers are compression molded to form sheets or blocks, which are then heat treated at high temperatures; the binding agent bonds the fibers together at contact positions. The fibers are preferentially orientated during the molding step, which can result in a material with highly anisotropic mechanical properties.

Low density ceramics within the range of interest are difficult to fabricate from powders since tap densities usually exceed the desired relative density of 0.1. Moreover, the ceramic further densifies during the heat treatment (sintering) used to bond the particles together. Sol-gel methods can produce very low density "particulate" networks when the liquid phase is removed above its critical point (super critical drying). Due to their high driving force for sintering, these low density macrostructures rapidly densify at moderate temperatures, and are thus not useful for high temperature applications.

Closed cell macrostructures are produced by either a foaming process or sintering hollow spheres.

Open cell macrostructures are currently produced by coating the connecting strut network of a reticulated, foamed polymer with a ceramic. The reticulated polymer substrate is manufactured by uniformly foaming a thermal setting polymer and then dissolving the thin cell walls. The substrate is coated with a ceramic powder, and, after drying, is eliminated by pyrolyzing



at moderate temperatures. After pyrolysis, the powder coating is densified by sintering at high temperatures. The reticulated polymer substrate can also be coated by a chemical vapor deposition method.

The mechanical properties of low density macrostructures and their relation to relative density and average macrostructural parameters has been a subject of relatively recent modeling and experimentation. Various models indicate that the elastic modulus can be expressed as:

$$E = A E_m (\rho / \rho_t)^n \quad (1)$$

where A is a constant, E_m is the elastic modulus of the material that forms the macrostructure, and ρ / ρ_t is the relative density. Simple models based on space filling unit cells suggest that the exponent n will depend upon whether structural units (bonded fibers or cell struts) flex when loaded and upon how the load is shared by various components of the macrostructure (e.g., cell struts vs cell walls). Gent and Thomas,¹ who neglected flexural deformation in cellular macrostructures, suggested that $n = 1.25$, which appears to be supported by data obtained on foamed glass.^{2,3} Gibson and Ashby,⁴ who include flexural deformation, suggest that $n = 2$ for open cell macrostructures and $n = 3$ for closed cell macrostructures. Green⁵ has shown that $n \sim 2$ when the cell wall thickness approaches 1/10 the cell strut dimension, a condition expected when, during fabrication, cell walls thin due to surface tension. Green⁶ has shown $n \rightarrow 2$ as hollow glass spheres sinter to develop a closed cell macrostructure. Green⁷ has also shown that $n = 2.6$ for tangled glass macrostructures.

The fracture toughness of various model macrostructures, as expressed by the critical stress intensity factor K_C , has been suggested to be related to the cell length (l), the cell strut (or fiber) strength (σ_f), and the relative density as:

$$K_C = B \sigma_f l^{1/2} (\rho / \rho_t)^m \quad (2)$$



were B is a constant, and the exponent m is expected to range between 1.3 (no flexing of structural units at the crack tip)⁶ to 1.5 (flexing of structural units occurs).^{8,9} Equations (1) and (2) can be combined to obtain:

$$K_C = C \alpha_f^{1/2} (E/E_m)^{m/n} \quad (3)$$

The strength (σ) of the low density ceramics is expected to obey the usual fracture mechanics relation:

$$\sigma = Y K_C / c^{1/2} \quad (4)$$

where Y is a constant dependent upon the mode of loading and crack geometry, and c is the size of the crack that gives rise to failure.

The major problem in fabricating a low density ceramic is producing a uniform macrostructure, and thus a material with uniform properties. For example, the mechanical properties of the tangled fiber macrostructures used in early Space Shuttle tiles were not only anisotropic (fiber orientation during molding caused the average strength of the strong direction to be twice that of the weak direction), but also variable between production units. The critical stress intensity factor, K_C , (determined in the weak direction) of different production units varied from the mean value by $\pm 35\%$.¹⁰ The strength distribution of this material is thus caused by both the statistical distribution of flaw sizes and the variation of the material's resistance to crack extension, as measured by the variation of K_C .

Because the uniformity of tangled fiber materials appears to be intrinsically limited by its fabrication method, the fabrication and properties of cellular macrostructures were studied. Green's⁷ study of the sintering of hollow glass spheres (initial relative density of spheres = 0.13; $69 \pm 6 \mu\text{m}$ diameter) showed that, although the uniformity of the closed cell macrostructure produced by this method was much greater than that for the



SC5364.2FR

tangled fiber macrostructures, large (200-500 μm), irregularly shaped voids were produced by the rearrangement forces that arise during sintering. Because the problem of void formation due to rearrangement is intrinsic to the nonuniform packing of particles, and thus to the sintering method, effort was redirected to the study of open cell macrostructures produced with reticulated, polymer foam precursors, whose cells did not appear to vary by more than $\pm 10\%$.

The purpose of this study was to determine the constraints of fabricating uniform, open cell macrostructures with relative densities < 0.1 by slurry coating foamed polymer substrates. This method is nearly unlimited by the chemistry of the resulting low density material. Pertinent mechanical properties (elastic modulus, strength, and fracture toughness) were measured as a function of cell size and related to flaws produced during fabrication.



2.0 EXPERIMENTAL PROCEDURE

2.1 Fabrication of Reticulated Macrostructures

Open celled macrostructures were fabricated by coating the struts of a reticulated polymer foam with a ceramic slurry, and then firing the resultant structure to pyrolyze the substrate and sinter the ceramic powder. Commercial reticulated polyurethane foams* with cell sizes ranging from 250 μm to 2.5 mm (100 to 10 pores per inch [ppi]) were used as substrates, which were coated with powder slurries of either alumina (Al_2O_3) or alumina/zirconia ($\text{Al}_2\text{O}_3/50 \text{ vol\% ZrO}_2 [+ 2.3 \text{ mol\% Y}_2\text{O}_3]$). Experiments were carried out to optimize the slurry conditions (volume fraction of solids, polymer additions, surfactant addition, etc.) for the coating of the polymer substrate. Procedures for strut coating, polymer pyrolysis, and powder sintering were also explored.

2.2 Property Determinations

The mechanical properties of reticulated ceramic macrostructures were measured for materials fabricated commercially.** The composition of these materials was identical to the $\text{Al}_2\text{O}_3/\text{ZrO}_2$ composites discussed above: 50 vol% ZrO_2 containing 3.0 mol% Y_2O_3 to retain the toughening tetragonal phase. The manufacturer agreed to fabricate, under conditions of best effort, specimens with a relative density not exceeding 0.1 of theoretical using substrates of 30, 65, and 100 ppi. Approximately one half of the specimens were specially processed by the manufacturer in an attempt to heal the cracks produced during polymer pyrolysis; these will be denoted as "healed" specimens.

The elastic modulus of each specimen was calculated from its sonic transmission velocity, according to the relationship:

* Scott Foam Division, Eddystone, PA.

** Hi-Tech Ceramics, Inc., Alfred, NY.



$$E = \rho V^2[(1 + \nu)(1 - 2\nu)/(1 - \nu)] \quad (5)$$

where ρ is the specimen's bulk density, V is the velocity of sound in the specimen, and ν is Poisson's ratio (assumed to be 0.2 for these materials). Sonic velocity was determined using a James V-Meter* by measuring the time required for a 150 kHz pulse to travel along the sample's long axis. Because the open cell surface was very rough, several measures were needed to assure good acoustic contact between the ceramic and the meter's transducer. The specimen ends were coated with epoxy, significantly smoothing the surface. The epoxy also impregnated the cells nearest the surface, ensuring intimate contact between the surface and the ceramic struts. A polymeric pad was then used to couple the specimen end to the transducer. The pad would flow to fill any remaining surface irregularities, creating good acoustic contact between the transducers and the sample surface.

The tensile strength of the specimens was determined using an Instron Universal Testing Machine** by loading at a constant crosshead rate of 0.05 cm/min. The specimens, which were nominally 25 by 25 by 50 mm, were epoxied to aluminum blocks to aid gripping by the test machine. To determine fracture toughness, double edge notch tests were performed on the larger piece of each fractured specimen. Using a diamond saw, the fracture surface was removed and the specimen was notched, perpendicular to the long axis, to a depth of between 3 and 6 mm, such that the total sample height was always at least 4 times the notch depth. The notched specimens were then tested in tension, using the same conditions as the strength tests. For this geometry, the fracture toughness, K_{IC} , is related to the tensile strength of the notched specimen, σ , by the relation:

* James Instruments, Inc., Chicago, IL.

** Model TM-M-L, Instron Corporation, Canton, MA.



SC5364.2FR

$$K_c = \sigma [\pi \ell]^{1/2} [1 + 0.122 \cos^4(\frac{\pi \ell}{2b})] [(\frac{2b}{\pi \ell}) \tan(\frac{\pi \ell}{2b})]^{1/2} \quad (6)$$

where $2b$ is the sample width and ℓ is the notch depth.



3.0 RESULTS

3.1 Fabrication of Reticulated Macrostructures

3.1.1 Pyrolysis of Polyurethane Foams

Figure 1 illustrates the weight loss of the polyurethane foam as a function of temperature (heating rate = 5°C/min). Pyrolysis occurs from 190°C to about 520°C in air and 430°C in nitrogen. Observations using a binocular microscope showed that, upon rapid heating, the polyurethane material softens, melts, and then boils.

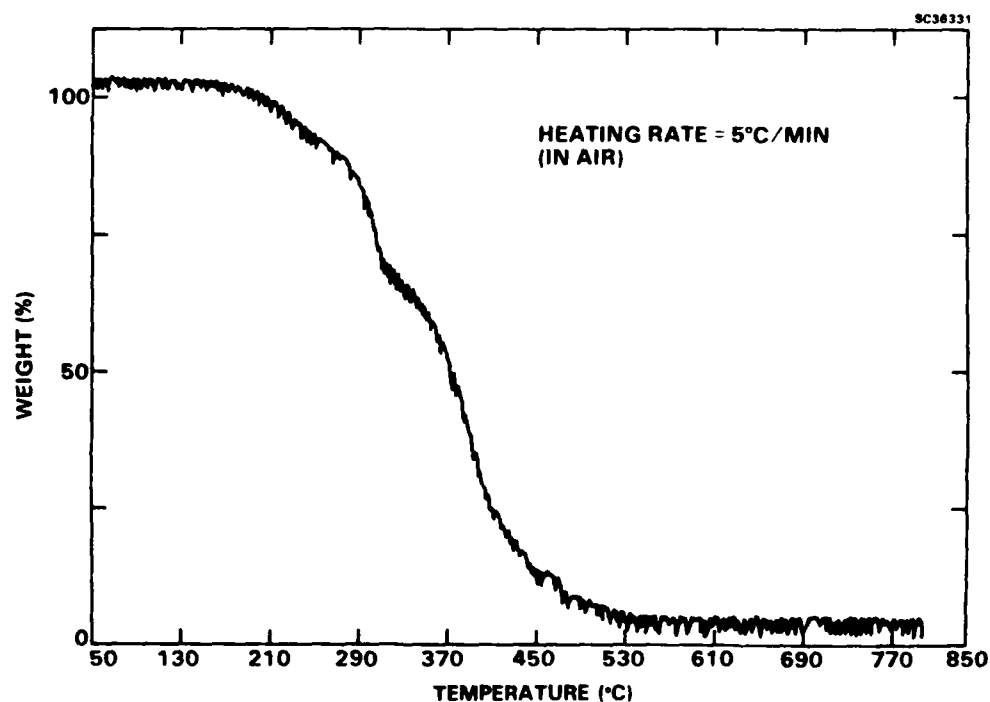


Fig. 1 Weight loss as a function of temperature (heating rate = 5°C/min) for pyrolysis of polyurethane foam in air.



3.1.2 Slurry Formulation

Dispersed, aqueous slurries were produced using a polyelectrolyte surfactant*. These slurries, which contained between 20 to 40 vol% solids, did not coherently coat the polyurethane substrates. Additions of polyethylene oxide (PEO, average molecular weight=100,000) were observed to produce a coherent coating. Extensive experimentation produced an optimum slurry formulation consisting of 40 vol% powder, 2 wt% surfactant, and 1 wt% PEO (wt% referenced to powder in slurry).

3.1.3 Substrate Coating Method

The reticulated polymer substrates acted like sponges and were sufficiently elastic to regain their shape after compression. To produce macrostructures with > 10% relative density, slurry could be incorporated into the reticulated substrates in the same manner that water is taken into a sponge: the substrates were compressed, immersed in the slurry, and allowed to expand. After immersion, excess slurry was squeezed out with a roller. Repeated rolling reduced the slurry content. To produce the lowest density macrostructures, a measured quantity of slurry was placed on one side of the polymer substrate, which was then rolled to redistribute the slurry. This process uniformly coated the polymer substrate.

In both cases, care had to be taken to prevent individual cells from retaining slurry. Cells that retained the slurry would shrink more than the surrounding cells during sintering, causing struts to collapse. Collapsed cells were a major uncontrolled flaw population within the ceramic macrostructure. Complete emptying of cells was most difficult to achieve for the polymer substrates with the smallest cell size (100 ppi).

* Darvon C.



SC5364.2FR

3.1.4 Densification of Ceramic Macrostructures

After drying, the slurry coated substrates were no longer compliant. Care had to be taken during handling to prevent the ceramic coating from flaking and breaking away from the substrate struts. For this reason, the coated substrates were dried on ceramic setters to avoid any handling after drying.

The coated substrates were heated to 1600°C in a schedule that minimized disruption during pyrolysis and allowed the ceramic to fully densify. This heating schedule consisted of a heating rate of 1°C/min to 550°C, rapid heating (2 h) from 550°C to 1600°C, and a 1 h hold at 1600°C.

Collapse of the substrates, due to the differential shrinkage of powder within filled cells, would occur after pyrolysis and during the initial sintering period, between 550°C and 1200°C. The severity of this problem was related to the number of filled cells within the specimen. As mentioned above, this problem could be prevented by properly coating the substrate to minimize the number of filled cells.

Densification of the ceramic powder caused the macrostructure to undergo a linear shrinkage strain of 23%, suggesting that the initial bulk density of the powder coating was 55% of theoretical. Figure 2 illustrates that the sintered $\text{Al}_2\text{O}_3/50 \text{ vol}\% \text{ZrO}_2$ coating is close to theoretical density. X-ray diffraction analysis showed that the tetragonal structure of the ZrO_2 was retained. Tetragonal ZrO_2 is the toughening agent in transformation toughened $\text{Al}_2\text{O}_3/\text{ZrO}_2$ composites.¹¹

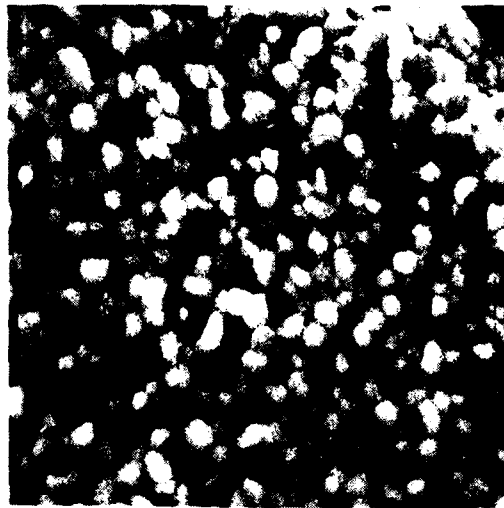
The lowest density macrostructure that could be produced was 3.9% of theoretical.

Figure 3 illustrates the ceramic struts of the typical low density reticulated macrostructure. The densified ceramic coating retains the general morphology of the polymer substrate. The struts, which are hollow due to substrate pyrolysis, have wall thicknesses between 10 and 30 μm . As shown in Fig. 4, all struts contain partial cracks caused by the disruptive pyrolysis



SC5364.2FR

SC36486



5 μm

Fig. 2 Microstructure of a densified $\text{Al}_2\text{O}_3/50 \text{ vol\% ZrO}_2$ strut.

SC36487



100 μm

Fig. 3 Macrostructure of a typical open cell reticulated ceramic fabricated using the slurry method.



SC5364.2FR

of the polymer substrate. Additionally, the pyrolysis frequently displaced strut walls from one other.

3.2 Properties of the Ceramic Reticulated Macrostructures

The mechanical properties of commercially fabricated $\text{Al}_2\text{O}_3/50 \text{ vol\% ZrO}_2$ (3.0 mol% Y_2O_3) reticulated ceramic macrostructures were measured. Fully dense material with compositions in this range can have a fracture toughness of $6.3 \text{ MPa m}^{1/2}$ and, when processed to minimize the size of various flaw populations, can have an average strength exceeding 2000 MPa. The elastic modulus of the fully dense material is 280 GPa.¹¹ X-ray diffraction analysis of these materials indicated that tetragonal ZrO_2 was retained during fabrication.

In general, the commercial material appeared similar to that processed in this laboratory. Macrostructures processed with the 100 ppi substrate frequently contained large regions of missing cells, presumably caused by slurry retention within the cells during the coating process. The integrity of the struts in the commercial material appeared better than that shown in Fig. 4, but cracks within the struts were still very frequent. Also, because of the higher relative density of the commercial material, the strut walls appeared thicker. Observations of the "healed" material indicated that some struts contained a second layer of material, as shown in Fig. 5. This observation suggests that the 'healed' ceramic macrostructures were recoated and fired a second time.

3.2.1 Elastic Modulus

Tables 1 and 2 list the average, maximum, and minimum values of elastic modulus and relative density for the six specimen sets: the "as-fabricated" and "healed" materials fabricated using 30 ppi, 65 ppi, and 100 ppi polyurethane precursors. As illustrated in Fig. 6 for the 65 ppi materials, the "healed" specimens had a higher modulus without a significant increase in density. This suggests that many of the cracks within the struts,



SC36488



20 μ m

Fig. 4 Partial cracks in a reticulated ceramic strut caused by substrate pyrolysis.

SC36489



1 mm

Fig. 5 Macrostructure of a commercially fabricated "healed" reticulated ceramic. Note the second ceramic layer caused by the recoating of the macrostructure.



SC5364.2FR

Table 1
Elastic Modulus Values for Each Specimen Set

Specimen Type (Pores Per Inch)	Elastic Modulus (GPa)		
	Average	Maximum	Minimum
30, as-received	2.04	2.46	1.33
30, healed	2.70	2.93	2.49
65, as-received	1.93	2.31	1.31
65, healed	2.88	3.27	2.55
100, as-received	1.64	2.95	0.96
100, healed	2.61	5.23	1.35

Table 2
Relative Density Values for Each Specimen Set

Specimen Type (Pores Per Inch)	Relative Density (% Theoretical Density)		
	Average	Maximum	Minimum
30, as-received	8.16	9.98	6.87
30, healed	8.88	9.18	8.60
65, as-received	9.23	9.76	8.24
65, healed	9.12	9.66	8.25
100, as-received	8.81	9.84	7.70
100, healed	9.95	11.94	8.78

which would decrease the elastic modulus, were eliminated by the "healing" process. Figure 6 also shows that the elastic modulus increases with relative density. Log-log plots of elastic modulus vs relative density for each set resulted in values for the exponent n in Eq. (1) ranging between 1 and 3.

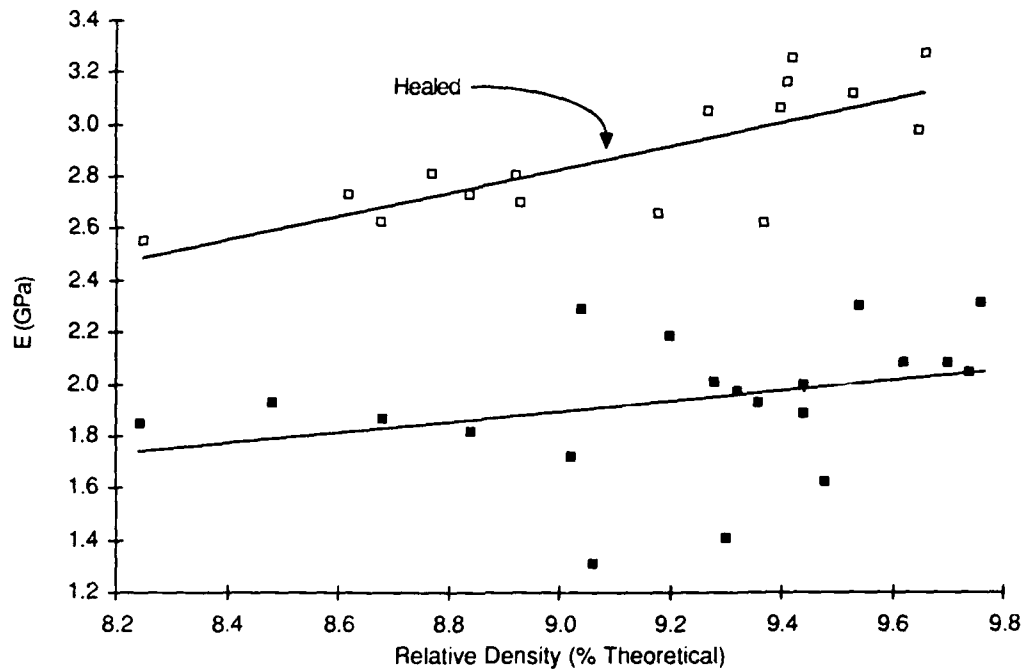


Fig. 6 Elastic Modulus as a function of relative density for commercial "healed" and "as-received" 65 ppi materials.

3.2.2 Fracture Toughness

Table 3 lists the average, highest, and lowest fracture toughness values for each of the six sets of specimens. Although average values of K_{IC} were not strongly affected by either cell size or the "healing" treatment, K_{IC} did increase with the elastic modulus, as suggested by Eq. (4) and shown for all data in Fig. 7. Data scatter prevented any conclusion concerning the value for the exponent in Eq. (4).

3.2.3 Tensile Strength

Table 4 lists the average, highest, and lowest values of tensile strength for each of the six sets of specimens. Strength as a function of fracture toughness is plotted for all data in Fig. 8. The scatter of the data suggests that the size of the fracture initiating crack is relatively independent of the material's cell size. Estimating the slope in Fig. 8 to be



SC5364.2FR

Table 3
Fracture Toughness Values for Each Specimen Set

Specimen Type (Pores Per Inch)	Fracture Toughness ($\text{kPa m}^{1/2}$)		
	Average	Maximum	Minimum
30, as-received	34.7	64.0	20.5
30, healed	34.5	50.2	15.6
65, as-received	35.5	52.1	20.3
65, healed	48.5	71.3	28.0
100, as-received	25.7	48.5	9.7
100, healed	29.8	76.1	7.9

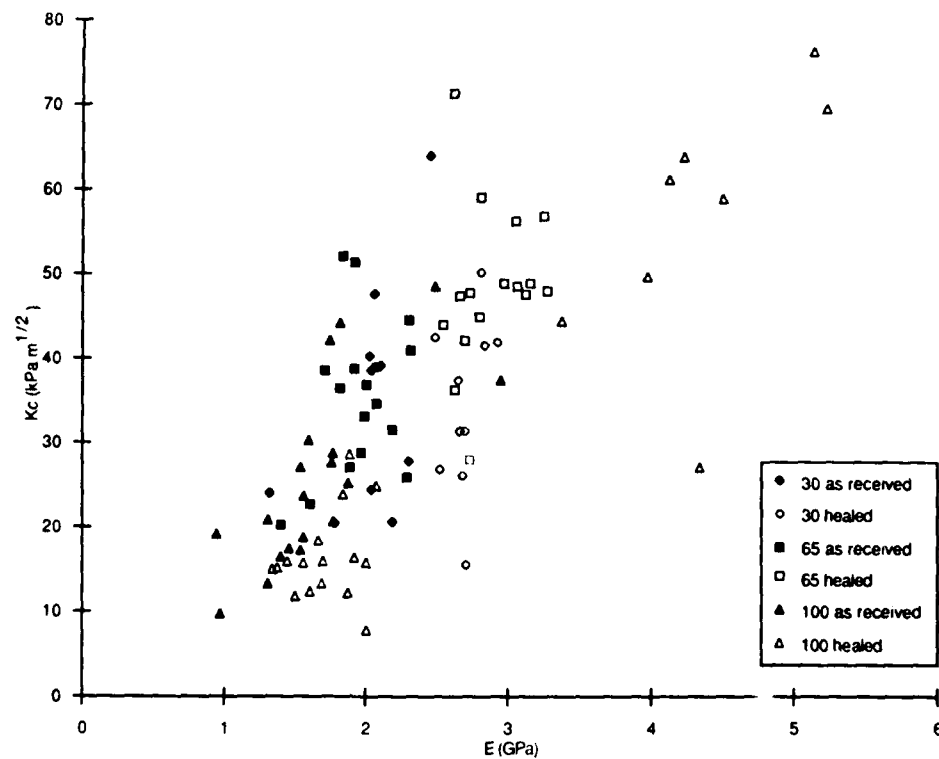


Fig. 7 Fracture toughness as a function of elastic modulus for all commercial specimens.



$10 \text{ m}^{-1/2}$, and using a value of $Y = 2.2 (\pi)^{-1/2}$ (half penny crack at the surface), Eq. (4) calculates the average fracture initiating crack size to be approximately 7 mm. Strut missing regions of this size were observed in some of the specimens fabricated using the 100 ppi polymer precursor.

Table 4
Tensile Strength Values for Each Specimen Set

Specimen Type (Pores Per Inch)	Tensile Strength (GPa)		
	Average	Maximum	Minimum
30, as-received	454	562	378
30, healed	422	535	277
65, as-received	456	651	116
65, healed	577	812	324
100, as-received	277	539	144
100, healed	282	678	93

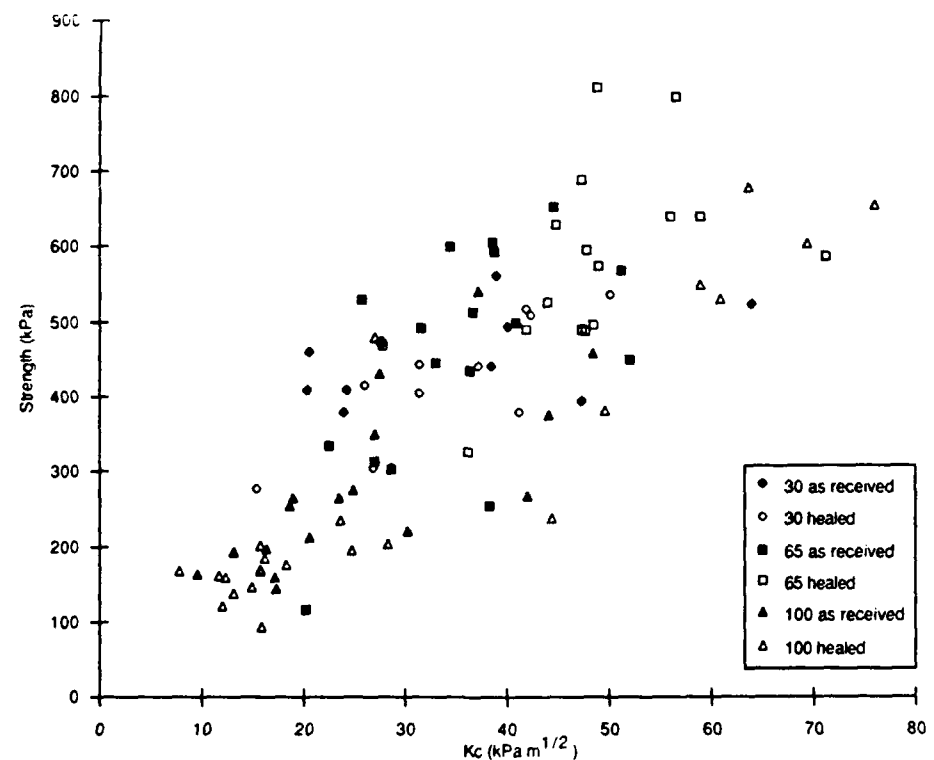


Fig. 8 Strength as a function of fracture toughness for all commercial specimens.



4.0 DISCUSSION

Obviously, the slurry coating method produces open celled macrostructures with far from optimum mechanical properties. Although this fabrication method is applicable to any material available as a powder, the disruptive processes that occur during polymer pyrolysis severely limit the strength of the cell struts and, therefore, the mechanical properties of the macrostructures themselves. In addition, the slurry process used to coat the reticulated polymer substrate can present problems as the cell size of the polymer precursor decreases, since it becomes increasingly difficult to prevent cells from retaining slurry.

Nevertheless, if a processing method which produces stronger struts could be developed, cellular ceramic macrostructures would have superior strength to density ratios. Methods which avoid the polymer substrate should be explored. One possibility might be to form the cellular macrostructure directly from a polymer-powder mixture. Conventional polymer foaming techniques could be applied to the filled polymer systems now used for the injection molding of ceramics. The powder would be incorporated into the strut itself, thus avoiding the disruptions of the coating currently associated with the substrate pyrolysis.



Rockwell International
Science Center

SC5364.2FR

5.0 ACKNOWLEDGEMENTS

The work was performed under contract to the Air Force Office of Scientific Research, Contract No F49620-83-C-0078.



SC5364.2FR

6.0 REFERENCES

1. A.N. Gent and A.G. Thomas, "Mechanics of Foamed Elastic Materials," Rubber Chem. Technol. 36, 597-610 (1963).
2. J.S. Morgan, J.L. Wood, and R.C. Bradt, "Cell Size Effects on the Strength of Foamed Glass," Mater. Sci. Eng. 47 [1], 37-42 (1981).
3. J.G. Zwissler and M.A. Adams, "Fracture Mechanics of Cellular Glass," pp 211-41 in Fracture Mechanics of Ceramics. Vol. 6 Ed. by R. C. Bradt, D. P.H. Hasselman and F.F. Lange, Plenum Press, NY (1980).
4. L.J. Gibson and M.F. Ashby, "The Mechanics of Three-Dimensional Cellular Materials," Proc. Roy. Soc. London, Ser. A. 382 [1782], 43-59 (1982).
5. D.J. Green, "Fabrication and Mechanical Properties of Lightweight Ceramics Produced by Sintering of Hollow Spheres," Report on AFOSR Contract No. F49620-83-C0078, June 1984.
6. D.J. Green, "Fabrication and Mechanical Properties of Lightweight Ceramics Produced by Sintering of Hollow Spheres," J. Am. Ceram. Soc. 68 [7], 403-409 (1985).
7. D.J. Green, "Fracture Toughness/Young's Modulus Correlations for Low-Density Fibrous Silica Bodies," J. Am. Ceram. Soc. 66 [4], 288-92 (1983).
8. M.F. Ashby, "The Mechanical Properties of Cellular Solids," Metall. Trans. A 14, 1755-69 (1983).
9. S.K. Maiti, M.F. Ashby, and L.J. Gibson, "Fracture Toughness of Brittle Cellular Solids," Scr. Metall. 18 [3], 213-17 (1984).



SC5364.2FR

10. D.J. Green and F.F. Lange, "Micromechanical Model for Fibrous Ceramic Bodies," J. Am. Ceram. Soc. 65 [3], 138-41 (1982).
11. F.F. Lange, "Transformation Toughening : Parts 1-5," J. Mat. Sci. 17, 225-262 (1982).

END

11-86

DT/C